Scattering of Conduction Electrons by Lattice Vibrations in Silicon

DONALD LONG
Honeywell Research Center, Hopkins, Minnesota
(Received August 4, 1960)

A theoretical model which assumes intervalley lattice scattering by phonons of 630° and 190°K characteristic temperatures in addition to the usual intravalley acoustic lattice scattering has been applied to the results of measurements of electrical conductivity, Hall effect, and weak-field magnetoresistance in the 30° to 350°K temperature range in samples of nearly pure *n*-type silicon. The model gives a good quantitative description of the results when the ratios of the coupling constants for the 630° and 190° phonons to the coupling constant for acoustic scattering perpendicular to an energy-spheroid axis are, respectively, about 2.0 and 0.15. The coupling constant for acoustic scattering parallel to a spheroid axis was found in an earlier study to be about 1.5 times that for the perpendicular direction. The magnitude of the acoustic contribution to the total lattice scattering mobility, as determined empirically here, is in approximate agreement with the predictions of deformation-potential theory.

I. INTRODUCTION

THIS paper reports an investigation in which the main objective has been to determine how accurately one can describe the magnitudes and temperature dependences of the various electrical transport effects in nearly pure *n*-type silicon by means of present theoretical ideas about lattice scattering in this material. It is now well known that the bottom edge of the conduction band in silicon is composed of six equivalent energy minima, or valleys, located at symmetrical positions within the Brillouin zone. Scattering by lattice vibrations can then be expected to cause two different types of electronic transitions; viz., transitions between states within a single valley (called intravalley acoustic-mode, or simply acoustic scattering throughout this paper), and transitions between states in different valleys (called intervalley scattering).[1] The acoustic scattering involves acoustic phonons of very low energy and is almost an elastic process. An intervalley scattering transition can be induced by the emission or absorption by an electron of a high-momentum, high-energy phonon, which can be of either acoustic- or optical-mode nature. Intervalley scattering can therefore be important only at temperatures high enough that an appreciable number of the suitable phonons are excited. The theoretical model to be applied to the experimental results describes the lattice scattering as a combination of these two mechanisms. A third conceivable lattice scattering mechanism would consist of intravalley transitions involving optical-mode phonons of low momentum but high energy (near the Raman frequency), but Harrison has shown that this mechanism is probably negligible in silicon.[2]

Two categories of information are required in order to make a sensible quantitative comparison between theory and experiment:

1. One must know the structure of the bottom edge of the conduction band, and in particular the number, shapes, and locations in k space of the valleys, to determine the wave-vectors σ of the phonons which take part in the intervalley scattering processes.

2. One must know the lattice vibrational spectrum to determine the energies of the intervalley phonons which have the required values of σ.

Rather complete knowledge of both these categories has recently become available for silicon. Actually, a third important category of information would be required to make the theory complete; viz., a knowledge of the strengths of the scattering by the various intervalley phonons and by the intravalley acoustic phonons, as represented by the various "coupling constants." The acoustic scattering coupling constant has been calculated, but the intervalley constants have not yet been worked out in full detail.[3] One of the primary objectives of this study has been to deduce approximate values for the intervalley coupling constants empirically by treating them as adjustable parameters in fitting the model to experimental results.

Reference should be made to the papers of Herring, Geballe, and Kunzler[4] for discussions of a number of basic theoretical and experimental considerations which are pertinent also to the present investigation. In order to extract the effects due alone to lattice scattering from those observed in the actual samples in which there is always some scattering by impurities, we have used the results of a recent study of impurity scattering in *n*-type silicon,[5] reference to which will be indicated as LM1 hereinafter. We have also made use of the conclusions in a recent paper on the anisotropies of the important scattering mechanisms in *n*-type silicon,[6] referred to as LM2. The essential features and results of the present project have been reported earlier.[7]

II. EXPERIMENTAL RESULTS

Measurements have been made of the electrical resistivity, Hall effect, and magnetoresistance as func-

[1] C. Herring, Bell System Tech. J. **34**, 237 (1955).
[2] W. A. Harrison, Phys. Rev. **104**, 1281 (1956).
[3] This point will be discussed further in Sec. V.
[4] C. Herring, T. H. Geballe, and J. E. Kunzler, Phys. Rev. **111**, 36 (1958); and Bell System Tech. J. **38**, 657 (1959).
[5] D. Long and J. Myers, Phys. Rev. **115**, 1107 (1959).
[6] D. Long and J. Myers, Phys. Rev. **120**, 39 (1960).
[7] D. Long and J. Myers, Bull. Am. Phys. Soc. **5**, 195 (1960).

tions of temperature, magnetic field strength, and crystallographic orientation on several samples of rather highly purified n-type silicon cut from single crystals grown by the floating-zone method. Details of sample preparation and purity and of measurement procedures have been given in LM2. Also, the magnetoresistance data have been reported in full in LM2. The most important data for our purposes here are those taken on the samples from the most nearly pure crystal, SP6, which had a concentration of electrically effective impurities of about 3×10^{13} atoms per cm^3.

Conductivity vs temperature data taken on sample SP6A between 100° and about 350°K are shown in Fig. 1. The carrier density is constant over this temperature range to within one percent, so that the data represent the temperature dependence of the electron mobility and are plotted as such. The open circles in Fig. 1 are theoretical values, not data points. There is no need to show the actual data points with the curve, since there would be no observable scatter in them on the scale of Fig. 1. The mobility is normalized to a value of about 1470 cm^2/volt-sec at 300°K to jibe with other results given later. Hall coefficient vs temperature data for SP6A over the same temperature range are shown in Fig. 2. Here, because of the constant carrier density, the data represent the temperature dependence of the Hall coefficient factor r, where the Hall coefficient $R_H=r/nq$ and n is the carrier density, and are plotted as such. The open circles are again theoretical values to be discussed later; the scale of r in Fig. 2 is normalized to fit these theoretical points, since the magnitude of r cannot be deduced unambiguously from the Hall coefficient. The Hall data were all taken at magnetic fields H weak enough that the "weak-field" ($H\rightarrow 0$) approximations in the theory of the effect should apply accurately. The importance of both Fig. 1 and Fig. 2 lies in the temperature dependences exhibited by the measured parameters, so that the particular normalization procedures used in establishing their magnitudes are not important at this stage. In both the above experiments sample SP6A had etched surfaces and six side-arm voltage probes.[6]

We have also done the above two types of experiments on several of the other samples listed in LM2; it is sufficient to point out that the results agreed with those for SP6A except for expected differences at the lower temperatures due to the stronger impurity scattering in the less pure samples.

III. THEORETICAL CONSIDERATIONS

As emphasized earlier, in order to make a sensible comparison between theory and experiment in the present study one must know (1) the structure of the bottom edge of the conduction band of silicon and (2) the lattice vibrational spectrum of silicon. We shall now discuss the available information on these subjects and how it applies in particular to the lattice scattering of electrons in silicon.

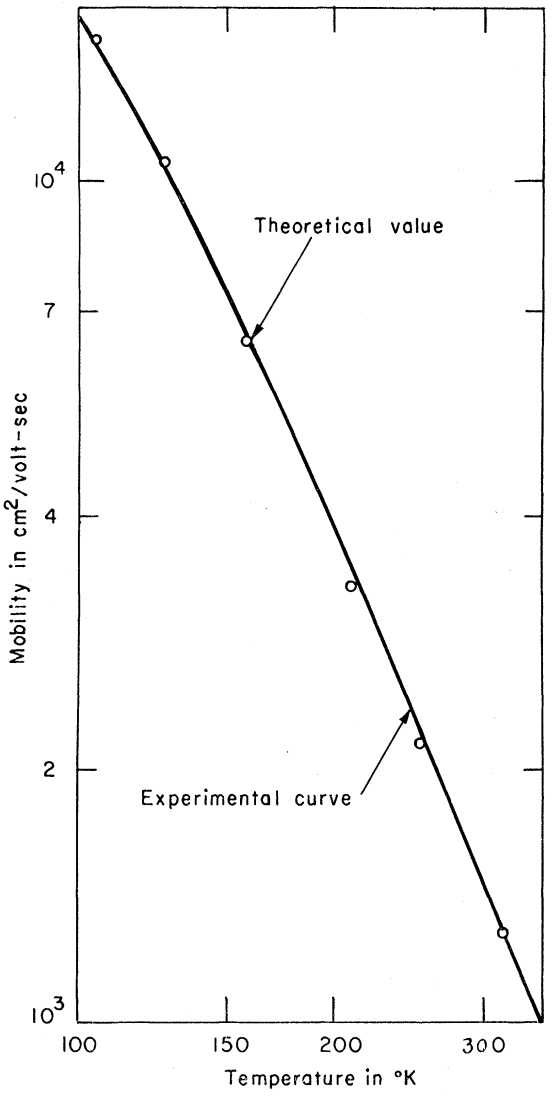

FIG. 1. Conductivity vs temperature on a log-log plot for sample SP6A. The ordinate represents the mobility and is shown as such, since carrier density is constant over this temperature range. The open circles are theoretical values, not data points.

Various experiments in the past few years have established that there are six valleys at the bottom edge of the silicon conduction band and that they are located on the [100] axes in k space at distances of 0.85 ± 0.03 of the way from the center of the Brillouin zone to its boundary.[1,8] The surfaces of constant energy at each valley are prolate spheroids. Figure 3 illustrates the situation by showing the first Brillouin zone for silicon and the positions of the valleys within it. The constant-energy spheroids are represented by equations of the form

$$\epsilon=\frac{\hbar^2}{2}\left(\frac{2k_\perp^2}{m_\perp}+\frac{k_\parallel^2}{m_\parallel}\right), \tag{1}$$

[8] G. Feher, Phys. Rev. **114**, 1219 (1959).

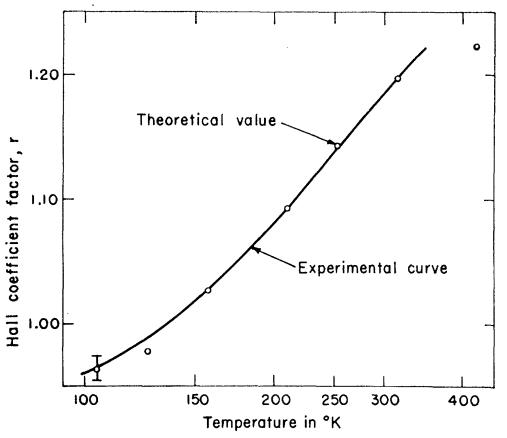

FIG. 2. Hall coefficient vs temperature on a semilog plot for sample SP6A. The ordinate represents the "Hall coefficient factor" and is shown as such, since carrier density is constant over this temperature range. The open circles are theoretical values, not data points.

where the k's are wave numbers, and $m_\perp$ and $m_{||}$ are the effective masses perpendicular and parallel, respectively, to the spheroid axis. Early cyclotron resonance experiments[9] established the mass values as $m_\perp=(0.19\pm0.01)m_0$ and $m_{||}=(0.98\pm0.04)m_0$, where m_0 is the mass of a free electron. Very recent cyclotron resonance experiments[10] give values of $m_\perp=(0.192\pm0.001)m_0$ and $m_{||}=(0.90\pm0.02)m_0$. The discrepancy in $m_{||}$ is as yet unexplained. We shall use the newer mass values throughout this paper and shall assume that they remain constant with increasing temperature up to $\sim$350°K. Under this assumption, for which there is some partial evidence of legitimacy,[10] none of the data will be explainable in terms of a change of mass with temperature or conduction electron energy.

The arrows in Fig. 3 indicate the possible intervalley scattering processes, of which there are two distinct types. One involves transfer of an electron in a [110]-type direction to any of four equivalent valleys (to be called "f scattering," after Morin, Geballe, and Herring[11]), and the other involves transfer of an electron in a [100]-type direction to the one remaining valley (called "g scattering"). It can be shown by simple geometrical arguments that both of these types of scattering must occur as Umklapp processes, in which the sum of the wave vector $\boldsymbol{\sigma}$ of the phonon and the change $\Delta\mathbf{k}$ of wave vector of the electron is equal to a principal vector of the reciprocal lattice, instead of simply equal to zero, for conservation of momentum. It also follows from geometrical considerations that all the wave vectors involved in both f and g scattering lie in [110]-type planes, so that the momentum conservation conditions can be illustrated by vector diagrams in a [110]-plane cross section of the reciprocal lattice of silicon, as is done in Fig. 4. It is important to note in Fig. 4 that the phonon involved in g scattering has its vector $\boldsymbol{\sigma}_g$ in a [100] direction and that the vector $\boldsymbol{\sigma}_f$ for f scattering is only about 11° off a [100] direction. Furthermore, $\boldsymbol{\sigma}_g$ has a magnitude of 0.30 of the maximum $\boldsymbol{\sigma}$ in the [100] direction, while $\boldsymbol{\sigma}_f$ is exactly equal to the maximum $\boldsymbol{\sigma}$ in its direction. The vector combinations shown in Fig. 4 are the only ones possible for single-phonon intervalley scattering for the known conduction band structure of silicon.

Now that the σ values of the intervalley phonons have been established, we can inquire into their energies. This information is contained in the lattice vibrational spectrum of silicon shown in Fig. 5, as determined recently by Brockhouse from neutron scattering experiments.[12] The spectrum in Fig. 5 is for [100]-directed phonons, and the phonon energies are plotted as equivalent temperatures, where $T=h\nu/k$, with ν the characteristic frequency. The transverse branches are doubly degenerate, so that there are actually six branches in all. The vertical marks on the branches at 0.3 of the way from the zone center to the boundary indicate the energies of the phonons involved in g scattering. Even though the f scattering phonons are not quite in the [100] direction, we feel that they are close enough that Fig. 5 should provide a good approximation to their energies, since the phonon spectrum should not change very rapidly with direction in the crystal. Under this assumption, the energies of the f-scattering phonons are given by the points at which the branches intercept the zone boundary.

It is important for the later analysis to note in Fig. 5 that the intervalley phonons fall within two ranges of energy which are rather widely separated. In terms of equivalent temperatures, these ranges are from about 135° to 220°K and from about 570° to 730°K. Thus, the allowed ranges of phonon energy are both considerably narrower than the gap between them. We point

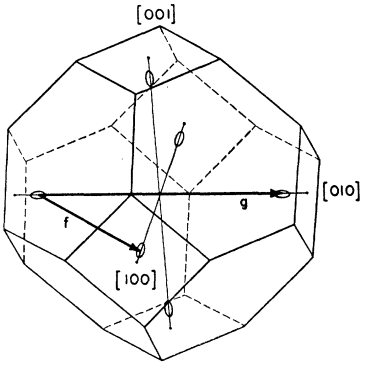

FIG. 3. Brillouin zone for silicon, showing positions of conduction band valleys. The arrows indicate the two possible types of intervalley scattering transitions.

[9] See, for example, R. N. Dexter, H. J. Zeiger, and B. Lax, Phys. Rev. **104**, 637 (1956).
[10] C. J. Rauch, J. J. Stickler, H. J. Zeiger, and G. S. Heller, Phys. Rev. Letters **4**, 64 (1960).
[11] F. J. Morin, T. H. Geballe, and C. Herring, Phys. Rev. **105**, 525 (1957).
[12] B. N. Brockhouse, Phys. Rev. Letters **2**, 256 (1959).

out in passing that the phonon which would be involved in any intravalley optical-mode scattering can be considered to fall within the upper phonon energy range, since its characteristic equivalent temperature is 735°K.

Herring[1] has indicated how one can treat intervalley scattering, once the relevant phonon energies are known, in terms of an expression for the relaxation time for combined acoustic and intervalley lattice scattering. The equation below is simply an extension of his expression to a general case in which there are several intervalley phonons of different energies and scattering strengths and in which the acoustic scattering may be anisotropic. Intervalley scattering is expected on reliable theoretical grounds to be isotropic.[1] Herring and Vogt[13] have shown that it is legitimate to describe the scattering by a relaxation time tensor diagonal in the principal axes of an energy spheroid for the types of scattering being considered in the present paper, so that there will be two relaxation times for n-type silicon, $\tau_\perp$ and $\tau_\parallel$.

$$\tau_\alpha=\left\{w_{A\alpha}\left(\frac{\epsilon}{kT_0}\right)^{\frac{1}{2}}\left(\frac{T}{T_0}\right)+\sum_i w_i\left(\frac{T_{ci}}{T_0}\right)^{\frac{3}{2}}\times\left[\frac{(\epsilon/kT_{ci}+1)^{\frac{1}{2}}}{\exp(T_{ci}/T)-1}+\frac{(\epsilon/kT_{ci}-1)^{\frac{1}{2}}\text{ or }0}{1-\exp(-T_{ci}/T)}\right]\right\}^{-1}. \quad (2)$$

The $w_{A\alpha}$ and w_i measure the strength of coupling of the electrons to acoustic and to intervalley phonons, respectively, and the subscript i ranges over all the intervalley phonons of different energies. The subscript α is to be replaced by $\perp$ or $\parallel$ depending on the direction relative to the spheroid axis. The temperatures T, T_{ci}, and T_0 are, respectively, the temperature at which the relaxation time is to be determined, the characteristic temperature of the ith phonon, and a reference temperature chosen to fix the magnitude of τ. The symbol ϵ represents the conduction electron energy. Equation (2) is the basic expression used in comparing theory and experiment, since all of the transport integrals describing the various effects are calculated as certain averages of the relaxation time components.[13]

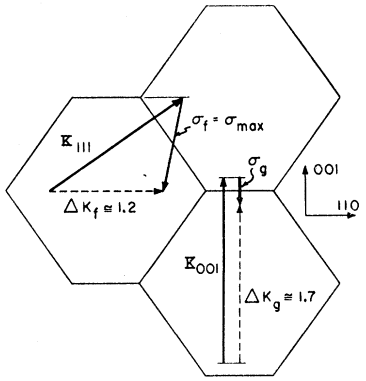

FIG. 4. [110]-plane cross section of several adjacent zones in silicon, showing the momentum conservation conditions for the intervalley scattering processes. $\bar{K}_{111}$ and $\bar{K}_{001}$ are principal vectors of the reciprocal lattice.

[13] C. Herring and E. Vogt, Phys. Rev. **101**, 944 (1956).

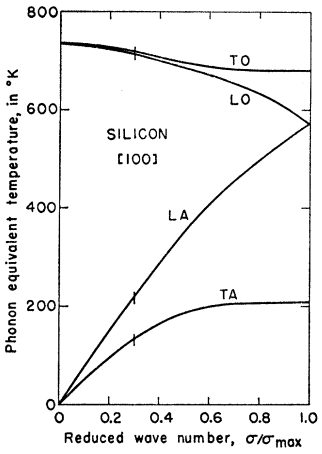

FIG. 5. Lattice-vibrational spectrum of silicon for [100]-directed phonons (after Brockhouse). The symbols *TO*, *LO*, *LA*, and *TA* indicate, respectively, transverse optical, longitudinal optical, longitudinal acoustic, and transverse acoustic branches.

IV. ANALYSIS OF RESULTS

Mobility vs Temperature

The initial and most basic problem is to fit the observed (drift) mobility vs temperature curve with a theoretical expression derived from the relaxation times of Eq. (2). Data are now available which indicate the shape of this curve fairly accurately from about 350° down to 30°K, provided use is made of some of the results in LM1, as well as the results in Fig. 1. It was found in LM1 that the lattice-scattering mobility (μ_{dL}) curve approaches the $T^{-1.5}$ behavior expected for acoustic scattering alone as the temperature is lowered to 30°K. By combining the results in LM1 for below 100°K with a μ_{dL} vs T curve deduced from Fig. 1, we have constructed the mobility vs temperature curve shown on a log-log plot in Fig. 6. The μ_{dL} values plotted in this curve have been calculated from the observed mobilities according to the procedure described in LM1 for subtracting out the impurity scattering contributions. This procedure involves determining μ_{dL} from the expression,

$$\mu_d=\mu_{dL}[1+x^2\{\mathrm{Ci}x\cos x+\mathrm{Si}x\sin x-\tfrac{1}{2}\pi\sin x\}], \quad (3)$$

where $x^2\equiv 6\mu_{dL}/\mu_{dI}$, $\mathrm{Ci}(x)$ and $\mathrm{Si}(x)$ are the cosine integral and sine integral, respectively, and the impurity scattering mobility μ_{dI} is calculated from the Brooks-Herring formula.[5,6] Equation (3) includes the condition that $\tau_L\propto\epsilon^{-\frac{1}{2}}$, where τ_L is the lattice-scattering relaxation time; this implies that only acoustic scattering is active, which would be strictly true only at the lowest temperatures. It turns out, however, to be a satisfactory assumption in the present situation where the correction for impurity scattering is very small at the higher temperatures at which other types of lattice scattering

are expected to be important. Further justifications for our manner of constructing Fig. 6 will come out of the analysis of this section.

It is interesting to compare the mobility values at the low-temperature end of Fig. 6 with the recent results of Rauch, Stickler, Zeiger, and Heller from their study of millimeter cyclotron resonance.[10] They deduced the relaxation time as a function of temperature from $\sim 1°$ to 50°K in an extremely pure silicon sample from measurements of line widths. At 30°K, for example, their results indicate a mobility of approximately 1.34×10^5 cm²/volt-sec. By assuming that the shape of their curve is determined by ordinary acoustic lattice scattering plus a small amount of ionized-impurity scattering, we estimate that their results give a lattice-scattering mobility of about 1.4×10^5 cm²/volt-sec at 30°K, as shown in Fig. 6. Taking account of possible experimental error in both cases, our results and theirs appear to be in very good agreement.

Our 30°K lattice-scattering mobility does not, however, agree with the value of about 8×10^4 cm²/volt-sec indicated by Logan and Peters in a recent paper on mobility in silicon.[14] The discrepancy occurs presumably because Logan and Peters made no correction for impurity scattering.

In order actually to compare theory and experiment, one must first calculate a mobility from the relaxation time of Eq. (2). The necessary relation is[13]

$$\mu_d=\frac{q}{3\langle\epsilon\rangle}\left[\frac{2\langle\epsilon\tau_\perp\rangle}{m_\perp}+\frac{\langle\epsilon\tau_\parallel\rangle}{m_\parallel}\right], \tag{4}$$

where the symbols $\langle\ \rangle$ represent Maxwellian averages, and the subscripts $\perp$ and $\parallel$ refer to directions perpendicular and parallel to the constant-energy spheroid axis. The procedure now is to substitute Eq. (2) into Eq. (4) and to adjust the intervalley coupling constants w_i to give the best fit of the resulting expression to the observed μ_{dL} vs T curve. In order to reduce the problem to reasonable proportions, since the fitting procedure requires many numerical integrations, we have chosen to assume that the possible contributions by all of the various intervalley phonons indicated in Fig. 5 can be approximated by just two such phonons, of energies equivalent to temperatures of 630° and 190°K. This approximation is reasonable, since, as pointed out already, all of the intervalley phonons lie within two rather narrow energy ranges, and these phonons approximately represent average energies of the two ranges. Any small amount of intravalley optical-mode scattering which may be present can be considered to be described by the 630° phonon, since the theoretical expressions for the intervalley and for the intravalley optical-mode scattering relaxation times are identical in form.[1]

One more piece of information is needed before we can proceed to the comparison of theory and experiment; viz., the anisotropy of the acoustic scattering relaxation time, as represented by the values of w_A in Eq. (2) for the $\perp$ and $\parallel$ directions. This anisotropy has already been found from the magnetoresistance experiments of LM2 to be in the vicinity of $w_{A\perp}/w_{A\parallel}=\frac{2}{3}$, and this is the value used in the subsequent analysis. Conduction in the "parallel" direction contributes only ten percent or less of the mobility (essentially because $m_\parallel \gg m_\perp$), so that the fit of theory and experiment in the μ_{dL} vs T curve is quite insensitive to the particular acoustic anisotropy.

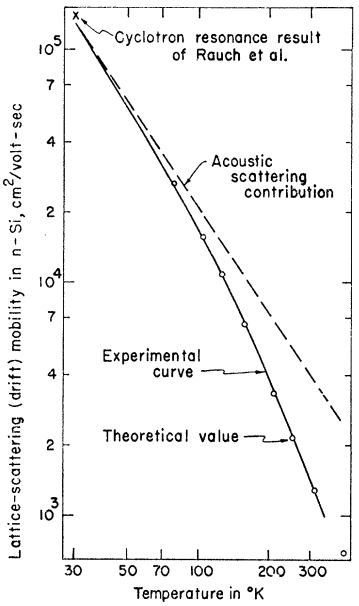

FIG. 6. Empirically derived mobility vs temperature curve for electrons in silicon, on a log-log plot. The open circles are theoretical values, not data points. The × at 30°K represents the mobility determined from the cyclotron resonance experiments of Rauch *et al.*

Now, in fitting theory to experiment one substitutes the expressions for $\tau_\parallel$ and $\tau_\perp$ derived from Eq. (2) into Eq. (4) and then adjusts $w_{A\perp}$, w_1, and w_2 (where w_1 is for the 630° phonon and w_2 is for the 190°K phonon) to give the best fit of the resultant form of Eq. (4) to the experimental curve over the entire 30° to 350°K temperature range. The magnitude of $w_{A\parallel}$ is of course already fixed relative to $w_{A\perp}$. Actually, $w_{A\perp}$ is the parameter which essentially fixes the absolute magnitude of the theoretical mobility to match the observed mobility at some reference temperature, while w_1 and w_2 adjust the shape of the theoretical curve. Thus, the values of w_1 and w_2 *relative* to $w_{A\perp}$ are of most interest to us now when dealing with the temperature dependence of the mobility, but we shall be equally interested later in this section in the theoretical implications of the observed magnitude of $w_{A\perp}$.

It becomes clear almost immediately upon trying to fit the theoretical μ_{dL} vs T expression to the experimental curve that scattering by the 630° phonon must be relatively strong, but that the 190° phonon must scatter only weakly. We have tried a number of combinations of values of w_1 and w_2 relative to $w_{A\perp}$ which satisfy this qualitative criterion and have found

[14] R. A. Logan and A. J. Peters, J. Appl. Phys. **31**, 122 (1960).

that the following ones give the best over-all fit:

$$w_1/w_{A\perp}=2.0, \quad w_2/w_{A\perp}=0.15.$$

The points shown in Fig. 6 are mobilities determined at representative temperatures by numerical evaluation of the relaxation time averages of Eq. (4) for the above values of the intervalley coupling constants. The dashed line with a -1.5 slope represents that part of the mobility contributed by the acoustic scattering.[1] It can be seen that the fit of theory to experiment is good to within a few percent. The fit is not particularly sensitive to the exact magnitudes of the coupling constants, but a change of $w_1/w_{A\perp}$ of, say, 15% would produce a noticeable worsening of the fit, as would a change of $w_2/w_{A\perp}$ of about a factor of 2.

We pointed out earlier in discussing the construction of the experimental curve of Fig. 6 that the ionized-impurity scattering had been subtracted out according to a procedure which included the assumption that only acoustic scattering is active, but that this procedure was legitimate because of the smallness of the impurity scattering at the higher temperatures where the assumption is poor. In order to verify this statement, we have calculated numerically the actual mobilities for sample SP6A at temperatures above 100°K by adding impurity scattering to the lattice scattering relaxation times already determined in connection with Fig. 6 according to the usual procedure, where $\tau_\perp^{-1}=\tau_{L\perp}^{-1}+\tau_{I\perp}^{-1}$, and similarly for the "parallel" direction. The magnitude of the impurity scattering relaxation time τ_I is calculated under the considerations of the Appendix of LM2 and with $\tau_{I\parallel}/\tau_{I\perp}\approx 4$. The resulting mobilities are plotted in Fig. 1 along with the experimental mobility curve for sample SP6A. The good fit provides justification for our method of constructing the μ_{dL} vs T curve of Fig. 6. The calculated mobility values in Fig. 1 are only slightly lower than those in Fig. 6, illustrating the minor importance of impurity scattering in sample SP6A.

This also shows that our neglect of scattering anisotropies in constructing Fig. 6 introduced no noticeable error above 100°K. Below 100°K there might be noticeable error, but it should still be small because of the predominance of the conduction in the perpendicular direction relative to an energy spheroid axis.

Hall Effect

The acoustic plus intervalley scattering model gives a satisfactory description of the temperature dependence of the mobility, but it is at least conceivable that some other scattering model might do just as well. It is therefore desirable to apply our model to other transport effects which are sensitive in different ways to the form of the scattering law. Let us then consider the Hall effect, as represented by the data of Fig. 2 for sample SP6A.

The particular parameter of interest is the Hall factor r, since it is the only part of the Hall coefficient sensitive to the scattering, and is furthermore the only part which depends on temperature above 100°K in sample SP6A. The Hall factor is related to the relaxation times and effective masses in the weak-field limit ($H\rightarrow 0$) by the following expression[13]:

$$r=\left(\frac{\langle\epsilon\rangle\langle\epsilon\tau_\perp^2\rangle}{\langle\epsilon\tau_\perp\rangle^2}\right)\frac{3\left[2\dfrac{\langle\epsilon\tau_\perp\tau_\parallel\rangle}{\langle\epsilon\tau_\perp^2\rangle}\left(\dfrac{m_\perp}{m_\parallel}\right)+1\right]}{\left[\dfrac{\langle\epsilon\tau_\parallel\rangle}{\langle\epsilon\tau_\perp\rangle}\left(\dfrac{m_\perp}{m_\parallel}\right)+2\right]^2}. \tag{5}$$

We have evaluated numerically the averages in Eq. (5) at various temperatures in the 100° to 350°K range for the same values of the intervalley coupling constants which gave the best fit to the mobility data. In this case, however, impurity scattering was added to the lattice scattering at each temperature according to the same prescription followed in calculating the theoretical points used in fitting the mobility data in Fig. 1. The points plotted as open circles in Fig. 2 represent the resulting values of r. Limits of error for strengths of impurity scattering 30% greater and smaller than that used are indicated at the lowest temperatures in Fig. 2 and show that the fit is quite insensitive to the strength of impurity scattering assumed. It is true for the Hall effect that about the same variations of the coupling constants from the values used as in the mobility case would also produce a noticeable worsening of the fit.

Weak-Field Magnetoresistance

The weak-field magnetoresistance is another effect to which we can apply the acoustic plus intervalley scattering model. The most convenient way to deal with this effect is in terms of the ratio of one of the weak-field magnetoresistance coefficients to the square of the Hall mobility (μ_H), which gives a dimensionless quantity. We have chosen the ratio which is related to the relaxation times and effective masses in the weak-field limit by the expression,[13]

$$\left.\frac{\Delta\rho/\rho_0 H^2)_{110}^{001}}{\mu_H{}^2}\right)_{H\rightarrow 0}=\left(\frac{\langle\epsilon\tau_\perp\rangle\langle\epsilon\tau_\perp{}^3\rangle}{\langle\epsilon\tau_\perp{}^2\rangle^2}\right)\left\{\frac{\left[\dfrac{\langle\epsilon\tau_\perp\tau_\parallel{}^2\rangle}{\langle\epsilon\tau_\perp{}^3\rangle}\left(\dfrac{m_\perp}{m_\parallel}\right)^2+\dfrac{\langle\epsilon\tau_\perp{}^2\tau_\parallel\rangle}{\langle\epsilon\tau_\perp{}^3\rangle}\left(\dfrac{m_\perp}{m_\parallel}\right)+1\right]\left[\dfrac{\langle\epsilon\tau_\parallel\rangle}{\langle\epsilon\tau_\perp\rangle}\left(\dfrac{m_\perp}{m_\parallel}\right)+2\right]}{\left[2\dfrac{\langle\epsilon\tau_\perp\tau_\parallel\rangle}{\langle\epsilon\tau_\perp{}^2\rangle}\left(\dfrac{m_\perp}{m_\parallel}\right)+1\right]^2}\right\}-1, \tag{6}$$

where $\Delta\rho/\rho_0 H^2)_{110}{}^{001}$ represents the fractional increase of resistivity in a field H parallel to the [001] axis when the current flows parallel to the [110] axis. If either of the other two independent coefficients were used instead, the combination of masses and relaxation-time averages would be somewhat different from that in Eq. (6), but the same averages would still be involved so that no new information would result.[13]

We have evaluated numerically the Maxwellian averages in Eq. (6) at temperatures covering the 195° to 273°K range in which the data fall (see LM2), again adding impurity scattering of a strength corresponding to sample SP6A according to the prescription used in the calculations for Figs. 1 and 2. Of course, some of the averages in Eq. (6) have already been determined in analyzing the mobility and Hall results. The same intervalley coupling constants as for Figs. 1 and 2 were again used. The results of these calculations are plotted as the open circles in Fig. 7, and the dashed curve through them is drawn simply to indicate the probable theoretical values between them and is therefore not an experimental curve.

The experimental results for sample SP6A at the weakest fields are represented by the ×'s in Fig. 7. These are values of the ratio

$$\frac{\Delta\rho}{\rho_0}\Big)_{110}^{001}\Big/\mu_H{}^2H^2,$$

where this magnetoresistance coefficient has been calculated from the ones actually measured on SP6A by the method described in LM2. Correction for the presence of voltage probe side-arms on SP6A has been made to $\mu_H{}^2H^2$ simply by invoking the $2\frac{1}{2}\%$ correction in the resistivity,[6] since the Hall coefficient R_H is not affected by the presence of side-arms integral with the sample[4] (note that $\mu_H=R_H/\rho$). We have not, however, made any side-arm correction to $\Delta\rho/\rho_0)_{110}{}^{001}$, but such a correction would be no larger than a couple of percent at most.[4] The principal interest here in which high accuracy is essential is in the temperature dependence. The magnitude of the weak-field magnetoresistance ratio of Eq. (6) is known to be difficult to determine to an accuracy of better than several percent because of its sensitivity to a number of sources of error, most of which are independent of temperature.

Figure 7 shows that the theory gives a good description of the weak-field magnetoresistance. This effect is not as sensitive to the values of the intervalley coupling constants as are the mobility and Hall effect vs temperature behavior, so that the apparent agreement between theory and experiment is not as significant here with respect to the particular values of the coupling constants. The magnitude of the ratio in Eq. (6) is generally relative sensitive, however, at any temperature to the form of the scattering law, so that the approximate agreement of magnitudes in Fig. 7 does

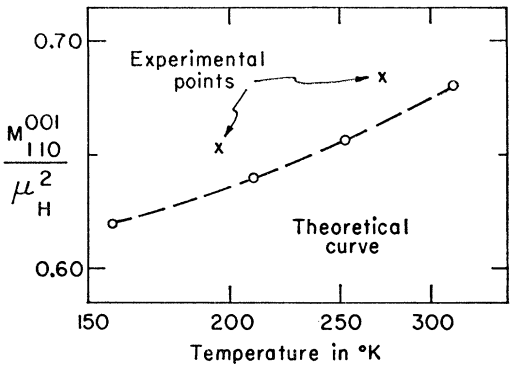

FIG. 7. Ratio of weak-field magnetoresistance coefficient $\Delta\rho/\rho_0 H^2)_{110}{}^{001}$ to square of Hall mobility $\mu_H{}^2$ vs temperature for sample SP6A. The data are represented by the ×'s. The open circles and the curve through them are theoretical results.

have some significance with respect to the validity of the acoustic plus intervalley scattering model.

The data for sample SP6X[6] are not plotted in Fig. 7, but the points would fall almost on top of those for SP6A. This is to be expected, since the two samples have approximately the same impurity scattering.

Magnitude of Mobility

One final point remaining to be considered is the relation between the observed mobility and theoretical predictions of its magnitude. This is actually the same as comparing the empirical value of the acoustic coupling constant $w_{A\perp}$ with theory, since the other coupling constants have already been determined relative to this one. Essentially, then, we want to compare the dashed line in Fig. 6, which represents the empirical acoustic contribution to the mobility, with theoretical predictions. This comparison can be made at any temperature, since the acoustic mobility follows a $T^{-1.5}$ law, and we have chosen 100°K.

Herring and Vogt,[13] and also Dumke,[15] have used deformation-potential theory to calculate the tensor component relaxation times $\tau_{A\parallel}$ and $\tau_{A\perp}$ for acoustic lattice scattering in terms of the effective masses, elastic constants, and a pair of deformation-potential constants. One of the deformation-potential constants can be determined from piezoresistance data and the other from a knowledge of the anisotropy of the relaxation time, as determined from magnetoresistance data. We shall not review their theory any further here, because it is clearly presented in all its details in their well-known papers. The essential results of it can be summarized in the form of two graphs in which are plotted the acoustic mobility μ_A and the relaxation-time anisotropy $\tau_{A\parallel}/\tau_{A\perp}$ as functions of the ratio Ξ_d/Ξ_μ of the two deformation potential constants. Herring and Vogt have presented plots of these types for a temperature of 100°K. Thus, by measuring the relaxation

[15] W. P. Dumke, Phys. Rev. **101**, 531 (1956).

time anisotropy (as we have done in the study reported in LM2) one can use these plots to deduce the value of μ_A predicted by the deformation-potential theory for that anisotropy. The result can then be compared with the empirical mobility for which we now have a value.

First, however, we must recalculate the μ_A vs Ξ_d/Ξ_μ curve to correspond with the scattering model and strength of the intervalley scattering we have been using. We shall give only a brief outline of the procedure, since it is treated in full detail in the papers by Herring and Vogt[13] and by Morin, Geballe, and Herring.[11] For n-type silicon, the contribution $m_{11}^{(p)}$ to the major piezoresistance coefficient due to redistribution of the conduction electrons among the six valleys when a strain destroys the cubic symmetry of the crystal can be shown to be related to the deformation-potential constant Ξ_u, to the mobilities of electrons parallel and perpendicular to each spheroid major axis (as limited by intravalley scattering mechanisms), and to the temperature T by

$$m_{11}^{(p)}=-\frac{2}{9}\frac{\Xi_u}{kT}\frac{(\mu_{11}-\mu_\perp)}{\mu}, \tag{7}$$

where μ is the resultant of μ_{11} and $\mu_\perp$. At the high temperatures where intervalley scattering is important, there is another contribution $m_{11}^{(I)}$ which is due to changes of intervalley scattering probabilities caused by strain. Thus

$$m_{11}(\text{observed})=m_{11}^{(p)}+m_{11}^{(I)}. \tag{8}$$

We ignore the minor effects which can give additional small contributions to m_{11}.

Now, the acoustic mobility is inversely proportional to Ξ_u^2, so that it is important to deduce the correct Ξ_u from the piezoresistance data for construction of the desired curve. These data are presented for several n-type silicon samples by Morin, Geballe, and Herring[11] in the form of a plot of m_{11} vs $1/T$ between about 60° and 250°K. In order to deduce Ξ_u from this plot we must (1) subtract the $m_{11}^{(I)}$ contribution from the high-temperature empirical values of m_{11} and (2) correct for the change with temperature of the quantity $[(\mu_{11}-\mu_\perp)/\mu]$ brought about by the increased influence of anisotropic impurity scattering at the lower temperatures. The theory of the $m_{11}^{(I)}$ term leads to an expression for the ratio, $m_{11}^{(I)}/m_{11}^{(p)}$, in terms of several Maxwellian averages of relaxation times, as given by Morin, Geballe, and Herring. We have evaluated these averages for the scattering model used throughout this section, and find that $m_{11}^{(I)}/m_{11}^{(p)}\cong 0.2$ at around 250°K. It should be noted that only f-scattering contributes to $m_{11}^{(I)}$, and that we have assumed that all the intervalley scattering around this temperature *is* f scattering in arriving at the above result. Actually, Ξ_u is not very sensitive to the value of the above ratio.

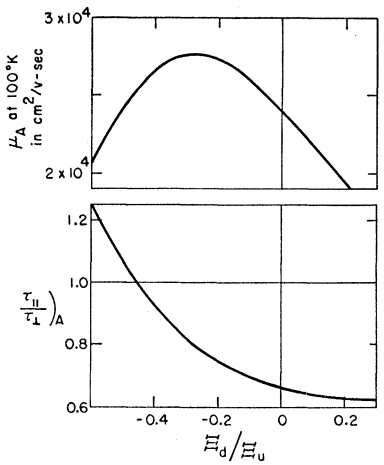

FIG. 8. Top curve: acoustic mobility μ_A at 100°K vs ratio Ξ_d/Ξ_u of the two deformation-potential constants for n-type silicon. Bottom curve: ratio of relaxation times for acoustic scattering parallel and perpendicular to a constant-energy spheroid axis vs Ξ_d/Ξ_u.

The change in $[(\mu_{11}-\mu_\perp)/\mu]$ between 250° and 60°K has been estimated for the samples studied by Morin, Geballe, and Herring, using the usual prescription for including impurity scattering ($\tau_{I11}/\tau_{I\perp}\approx 4$), and has been found to be about 6%, with the smaller value occurring at the lower temperature.

Invoking both these corrections, we find that $m_{11}^{(p)}=-(25\,000)/T+\text{const}$. This compares with a value of

$$m_{11}^{(p)}=-(24\,700)/T+\text{const}$$

used by Herring and Vogt[13] in constructing their μ_A vs Ξ_d/Ξ_u curve in which they assumed some intervalley scattering at the higher temperatures. Our result then leads to the curve shown in Fig. 8, in which the τ ratio vs Ξ_d/Ξ_u relationship is also shown. The most recent cyclotron resonance masses have been used in constructing Fig. 8. The other input data were the same as used by Herring and Vogt.

The empirical acoustic scattering relaxation-time anisotropy of $\tau_{A11}/\tau_{A\perp}\approx\frac{2}{3}$ deduced in LM2 under the assumption that the latest cyclotron resonance masses are correct is seen to correspond in Fig. 8 to a mobility of about 24 000 cm²/volt-sec. The empirical mobility has a value from Fig. 6 of about 21 000 cm²/volt-sec at 100°K. Thus, the theoretically predicted and empirically deduced mobilities agree to within about 15%, which is considered good in view of the pronounced sensitivity of the mobility to the τ ratio in the vicinity of $\tau_{A11}/\tau_{A\perp}=\frac{2}{3}$ and also in view of the uncertainty as to the exact value of the empirical τ_A ratio.[6] Note, however, that if the older cyclotron resonance masses were assumed correct, the $\tau_{A11}/\tau_{A\perp}$ ratio would be approximately 10% larger than $\frac{2}{3}$, thereby increasing the discrepancy. The μ_A curve would be shifted upward also, but only slightly.

V. CONCLUSION

The acoustic plus intervalley scattering model used here has been found to give a good general description of the lattice scattering of electrons in silicon from 30° to 350°K. The model does not give a truly precise quantitative description of all the experimental results, but of course small quantitative discrepancies are to be expected as a result of the various assumptions and simplifications included in the model.[16] The values deduced for the intervalley coupling constants must be considered merely as *approximate* representative averages, not necessarily as true values for real phonons. Thus, our conclusion is that the acoustic and intervalley mechanisms, as defined here, are very probably the only significant lattice scattering mechanisms for electrons in silicon, as had been expected for the known structure of the silicon conduction band.

Throughout this paper, we have treated the intervalley coupling constants as adjustable parameters to be determined empirically. Dumke has very recently made what are believed to be the first calculations of intervalley coupling constants for silicon.[17] His calculations were in connection with a study of the low-temperature recombination radiation spectrum of silicon. Dumke finds that at 300°K, intervalley phonons with characteristic temperatures of about 530° and 270°K contribute 22% and 56%, respectively, to the total scattering of electrons, the remainder being intravalley acoustic scattering. These characteristic temperatures are in reasonable agreement with the picture presented in Sec. III, which is not surprising, but the above strength of scattering for the lower energy phonon is in rather violent disagreement with our experimentally derived conclusion that this phonon must scatter only weakly. We have no explanation for the discrepancy.

Another important result of the present study is that the empirically deduced acoustic contribution to the lattice scattering mobility has been found to agree fairly well with the predictions of deformation-potential theory, particularly if the most recently measured effective masses are the correct ones. It should be realized, however, that this particular subject could use further investigation, since the acoustic scattering anisotropy and other pertinent parameters are not yet very well established quantitatively.

[16] It is possible that discrepancies somewhat larger than any apparent in Figs. 1, 2, and 6 would appear at temperatures above 350°K. Mobility vs temperature curves for samples with greater impurity concentrations than those reported here, which therefore exhibit extrinsic conduction to higher temperatures, have shown no decrease of slope (on the log-log plot) at the higher temperatures; whereas, the theoretical model used here predicts a gradual decrease above 350°K (see Fig. 6).

[17] W. P. Dumke, Phys. Rev. **118**, 938 (1960).

ACKNOWLEDGMENTS

The writer is greatly indebted to Mrs. E. Swedberg for carrying out the greater part of the many numerical evaluations of Maxwellian integrals and to J. Myers for assistance with all of the experimental aspects of the project.